# HYDROLYTIC DEGRADATION AND BIOACTIVITY OF LACTIDE AND CAPROLACTONE BASED SPONGE-LIKE SCAFFOLDS LOADED WITH BIOACTIVE GLASS PARTICLES

**A.Larrañaga[a], P. Aldazabal[b], F.J. Martin[b], J.R.Sarasua[a,*]**

[a] University of the Basque Country (UPV/EHU), Department of Mining-Metallurgy Engineering and Materials Science & POLYMAT, School of Engineering, Alameda de Urquijo s/n, 480130 Bilbao, Spain.

[b] Donostia University Hospital (Osakidetza-Basque Health Service) & BIODONOSTIA, Donostia-San Sebastián, Spain.

This is the accepted manuscript of the article that appeared in final form in **Polymer Degradation and Stability** 110 :121-128 (2014), which has been published in final form at https://doi.org/10.1016/j.polymdegradstab.2014.08.021. 

* Corresponding authors. Phone: +0034 946 014 271.

Fax: +34-94-601-3930.

E-mail: jr.sarasua@ehu.es (J.R. Sarasua).

**Abstract**

Bioresorbable highly porous polymer scaffolds play a pivotal role in tissue engineering applications. Ideally, the degradation rate of these scaffolds should match the tissue regeneration rate so that there is a gradual transfer of mechanical loads from the scaffold to the regenerated tissue. In this study the degradation behavior of porous and non-porous poly(L-lactide) (PLLA), poly(ε-caprolactone) (PCL) and poly(lactide-co-ε-caprolactone) (PLCL) in phosphate buffered saline (PBS) at 37 ºC for a period up to 18 weeks was investigated. The calculated degradation rates ($K_{Mw}$) of the samples studied, from the fastest to the slowest, was: PLCL>PLLA>PCL. On the other hand, the porous structures displayed slower degradation rates with respect to their non-porous counterparts. Finally, the bioactivity of a porous PLLA scaffold filled with 0, 15 and 30 vol.% of bioactive glass particles was confirmed by the deposition of an apatite layer on the surface of the material. Even in the scaffold filled with 15 vol.% of bioactive glass particles the precipitation of the apatite layer was observed in 14 days, whereas in the scaffold with 30 vol.% of bioactive glass this layer appeared just 3 days after being submerged in simulated body fluid (SBF).

Keywords: poly(L-lactide), poly(ε-caprolactone), poly(lactide-co-ε-caprolactone), hydrolytic degradation, bioactive glass.

## 1. Introduction

Tissue engineering is defined as an interdisciplinary field that applies the principles of engineering and life sciences in the development of biological substitutes that restore, maintain or improve tissue functions [1]. For the reconstruction of critical size bone defects, that is those that do not heal spontaneously and are filled with fibrous connective tissue instead of new bone [2, 3], tissue engineering is considered as a promising alternative to the autografts and allografts that are currently employed. In this sense, metallic, ceramic or polymeric scaffolds, alone or in combination with cells, can be satisfactorily employed to promote bone regeneration and facilitate the reconstruction of critical size defects [4-9].

Ideally, the scaffolds used for bone tissue engineering should have a three-dimensional, highly porous structure with an interconnected pore network that allows cell growth and at the same time permits the flow of nutrients and metabolic waste [10]. The materials used for the creation of these scaffolds should also be biocompatible and bioresorbable, displaying a controllable degradation and resorption rate that matches the cell/tissue growth *in vitro* and/or *in vivo*. Synthetic biodegradable polyesters, such as poly(L-lactide) (PLLA) and poly(ε-caprolactone) (PCL), are of great interest in this field because of their biocompatibility, biodegradability and the ease with which they can be formed into complex shapes. These polyesters undergo bulk degradation in aqueous environments due to the random-scission of their ester linkages [11]. It is well known, however, that crystalline regions in the polymer structure are highly resistant to hydrolytic degradation in regard to amorphous regions and thus, the degradation and reabsorption rates of these homopolymers are relatively slow due to their high crystallinity.

To overcome this problem, lactide and caprolactone based copolymers (PLCL) with reduced crystallization capability are being developed [12, 13]. Depending on their composition and chain microstructure the crystallization capability of lactide and caprolactone units is reduced giving rise to materials with higher degradation rates.

The lack of bioactivity of the polymers mentioned above can be a disadvantage in some medical applications. For this reason composite systems made of biodegradable polymers filled with bioactive particles are arousing interest, particularly in bone tissue engineering applications. Among the available inorganic bioactive particles, bioactive glasses (e.g., Bioglass45S5) present a rapid bone bonding and are therefore considered as Class A bioactive materials [14]. Bioactive glass is an osteoproductive and osteoconductive material. In contrast to Class B bioactive materials it also forms a chemical/biological bond with soft tissues, avoiding any relative movement (micromotion) of the implanted material and provides an improved long-term survival period for the implant [15]. The dissolution products of bioactive glass have a direct effect on the deposition of a hydroxyl carbonate apatite layer on the surface of the material [16] and on the gene-expression profile of surrounding cells [17], inducing osteoblast proliferation and differentiation. Recent studies have also reported the pro-angiogenic properties of bioactive glass filled polymeric scaffolds, leading to greater vascularization and a higher percentage of blood vessels in the constructs [18].

In this work, sponge-like scaffolds of PLLA, PCL and PLCL containing 0 or 15 vol.% of bioactive glass particles were prepared by solvent casting/particulate leaching and their hydrolytic degradation behaviour was compared to the degradation behaviour of their non-porous counterparts in phosphate buffered saline (PBS) for a period up to 18 weeks. Molecular weight, thermal transitions and mass loss were monitored during the *in vitro* degradation study by means of gel permeation chromatography (GPC),

differential scanning calorimetry (DSC) and weight measurements. Finally, the bioactivity of a PLLA scaffold filled with 0, 15 and 30 vol.% of bioactive glass was evaluated, with the formation of a Ca-P deposition on the surface of the composites after being submerged in simulated body fluid (SBF) at 37 ºC being monitored. The Ca-P deposition was characterized by means of X-ray diffractometry (XRD), Fourier transform infrared spectroscopy (FTIR) and scanning electron microscopoy (SEM).

## 2. Materials and methods

### 2.1. Materials

PLLA of a weight average molecular weight ($M_w$) of 160,000 and polydispersity index (PDI) of 1.70, PCL of a $M_w$ of 120,000 and PDI of 1.61 and PLCL of LA/CL molar weight ratio approximately 70/30, a $M_w$ of 190,000 and PDI of 1.67, were kindly supplied by Purac Biochem (The Netherlands).

The 45S5 Bioglass® particles were kindly supplied by Novabone® (US). The composition of Bioglass® (in wt.%) was 45.0% $SiO_2$, 24.4% $Na_2O$, 24.5% CaO and 6.0% $P_2O_5$. The size of the particles was <60 µm, with a mean particle size of 9 µm, with a density of 2.75 g $cm^{-3}$. The particles were dispersed in ethanol to measure their size distribution and after sonicating for 15 minutes a few drops were placed on a microscope glass slide. Finally, the sample was examined in a microscope and the size distribution was determined using ImageJ software.

### 2.2. Preparation of the samples

Porous scaffolds were prepared by solvent casting/particulate leaching using chloroform (Panreac, Spain) as solvent and NaCl (Sigma Aldrich, Spain) particles (200-355 µm) as porogen. Briefly, a dissolution of polymer in chloroform was mixed with salt particles

in a 1:9 polymer to salt weight ratio. In the case of scaffolds loaded with bioactive glass particles, 15 or 30 vol.% of particles were added to the mixture and then ultrasonicated for 15 minutes to obtain an homogeneous distribution of bioactive particles in the solution and to avoid the formation of agglomerates. Finally, they were transferred to a square Teflon mold (100 x 100 $mm^2$) and after evaporation of the chloroform, sheets of ~1.2 mm were obtained. Circular samples of 10 mm in diameter were punched out from these sheets and placed in distilled water for 48 h to leach out the salt particles. In the case of non-porous films no salt was added during the manufacturing and the final films had a thickness of ~0.2 mm.

### 2.3. Hydrolytic degradation study

For the hydrolytic degradation study, samples (initial weight, $W_0 \approx 20$ mg) were placed in Falcon tubes containing phosphate buffered saline (PBS) (pH = 7.2, Sigma-Aldrich, Spain) maintaining a surface area to volume ratio equal to 0.1 $cm^{-1}$. The samples were then stored in an oven at 37 ºC. At different periods of time (0, 3, 7, 14, 28, 42, 55, 76, 104, 132 days), three samples from each group were removed from the PBS and weighed wet ($W_w$) immediately after wiping the surface with a filter paper to absorb the surface water. These samples were air-dried overnight and vacuum-dried for another 24 h. After this they were weighed again to ascertain the dry weight ($W_d$). Water absorption (%WA) and remaining weight (%RW) were calculated according to equations 1 and 2:

$$\%WA = \frac{W_w - W_d}{W_d} \cdot 100 \quad (1)$$

$$\%RW = \frac{W_d}{W_0} \cdot 100 \quad (2)$$

The pH of the medium was measured using a pH-meter (HANNA, HI-8314).

The molecular weight of the samples was determined by GPC using a Waters 1515 GPC apparatus equipped with two Styragel columns ($10^2$ - $10^4$ Å). Chloroform was used as an eluent at a flow rate of 1 mL $min^{-1}$ and polystyrene standards (Shodex Standards, SM-105) were used to obtain a primary calibration curve. Samples containing bioactive glass were filtered prior to analysis using syringe filters (Acrodisc®, 0.45 µm, Waters).

The thermal properties were determined on a DSC 2920 (TA Instruments). Samples of 5-10 mg were heated from -90 to 210 ºC at 20 ºC $min^{-1}$. This first scan was used to determine the melting temperature ($T_m$) and the heat of fusion ($\Delta H_f$) of the polymers. After this first scan, the samples were quenched in the DSC and a second scan was collected from -90 to 210 ºC at 20 ºC $min^{-1}$. In this second scan the glass transition temperatures ($T_g$) were determined from the inflection point of the heat flow curve.

**2.4. Bioactivity study**

For the bioactivity study, porous PLLA scaffolds filled with 0, 15 and 30 vol.% of bioactive glass were submerged in simulated body fluid (SBF) at 37 ºC and at a surface area to volume ratio equal to 0.1 $cm^{-1}$. SBF, with solution ion concentrations similar to those of blood plasma [19], was prepared by dissolving reagent-grade chemicals of NaCl, $NaHCO_3$, KCl, $K_2HPO_4 \cdot 3H_2O$, $MgCl_2 \cdot 6H_2O$, $CaCl_2$, $Na_2SO_4$ and buffered at a pH value of 7.4 at 37 ºC with tris-(hydroxymethyl aminomethane) [$(CH_2OH)_3CNH_2$] and hydrochloric acid (HCl). Complementary studies [20] indicate that the SBF must be changed regularly because the concentration of cations decreases during the experiments owing to chemical change in the samples. In this study the SBF was changed every 3 days.

At different periods of time (0, 3, 7, 14 and 28 days), three samples from each group were taken out of the SBF and rinsed in abundant deionized water before drying at room temperature for 24 h and a further 24 h in vacuum.

The Ca-P layer that developed on the surface of samples was characterized using scanning electron microscopy (SEM) (HITACHI S-3400). Samples were fractured after being frozen in liquid nitrogen. Then they were coated with a 150 Å layer of gold in a JEL Ion Sputter JFC-1100 at 1200 V and 5 mA.

The chemistry of the mineral layer formed was examined using a Fourier transform infra-red spectrometer (FTIR). A small amount of powder was scratched from the surface of the incubated samples and then milled with KBr and pressed into a disc. Infrared spectra of these samples were recorded on a Nicolet AVATAR370 FTIR. Spectra were taken with a resolution of 2 $cm^{-1}$ and were averaged over 64 scans. The absorbance of all the studied samples was within the range where the Lambert-Beer law is obeyed.

The formation and crystallization of hydroxyapatite was confirmed by means of X-ray difrafctometry (XRD). The X-ray powder diffraction patterns were collected by a PHILIPS X´PERT PRO automatic diffractometer operating at 40 kV and 40 mA, in theta-theta configuration, secondary monochromator with Cu-Kα radiation (λ = 1.5418 Å) and a PIXcel solid state detector. Data were collected from 10 to 50º 2Θ (step size = 0.026 and time per step = 0.8 s/channel) at room temperature. A fixed divergence and anti-scattering slit to produce a constant volume of sample illumination were used.

## 3. Results and discussion

### 3.1. Hydrolytic degradation study

*3.1.1. Hydrolytic degradation of non-porous samples*

Figure 1 displays the DSC curves of the first scans of non-porous PLLA, PCL and PLCL samples at different degradation times. PLLA is a semi-crystalline polymer, showing a melting peak at ~166 ºC and an initial crystallinity fraction ($X_c$) of 35%, which was calculated using equation 3:

$$X_c = 100\ \Delta H_f / \Delta H^0_f\ (LA^*) \quad (3)$$

where $\Delta H_f^0$ = 106 (J $g^{-1}$ of PLLA) is the enthalpy of fusion of PLLA crystals having the infinite crystal thickness [21] and (LA*) is the actual lactide mass fraction in the (co)polymer (equal to 1 in the case of PLLA). As degradation occurred the $X_c$ of PLLA gradually increased and reached 58% at day 132. These changes in PLLA are related to the reduction in molecular weight which brings about a decrease in molecular entanglement and an increase in chain mobility. Because of this higher mobility, the chains could reorganize themselves to a more orderly macromolecular arrangement and therefore, the crystallinity of PLLA increased [22]. Moreover, since the hydrolysis occurs preferentially in amorphous regions [23], an increase in the crystallinity fraction of PLLA samples over time was expected.

PCL is also a semi-crystalline polymer with melting point of ~64 ºC and an initial $X_c$ of 59%, which was calculated using equation 4:

$$X_c = 100\ \Delta H_f / \Delta H^0_f \quad (4)$$

where $\Delta H_f^0$ = 142 (J $g^{-1}$ of PCL) is the enthalpy of fusion of PCL crystals having the infinite crystal thickness [24]. In contrast to PLLA, the $X_c$ of the PCL samples stayed more or less constant throughout the degradation study.

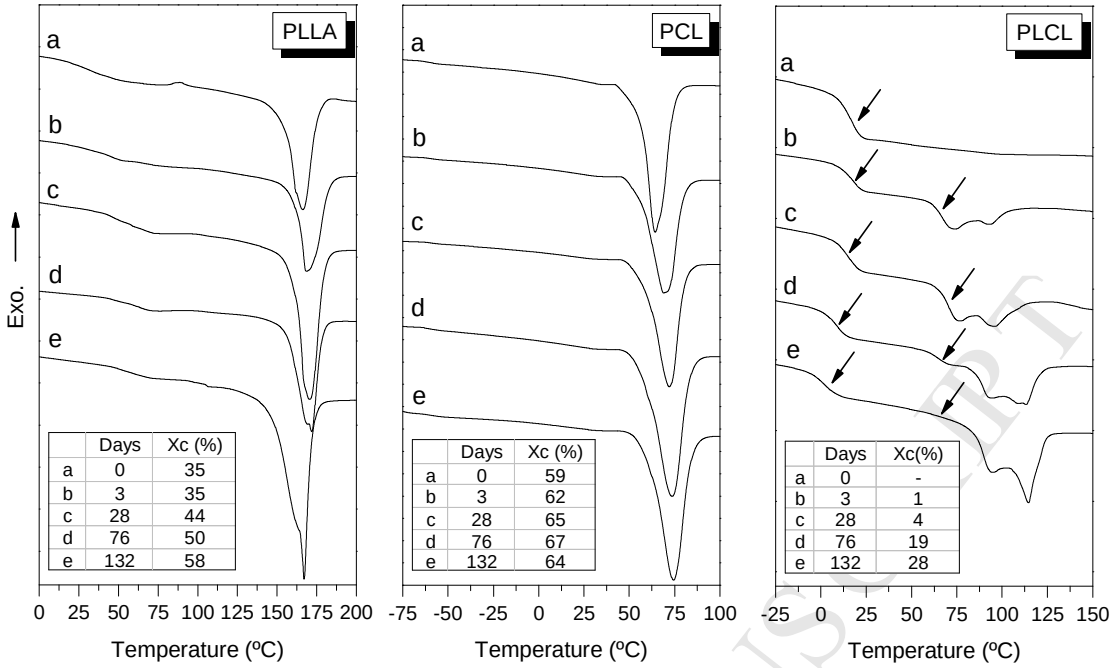


**Figure 1.** First DSC scans of non-porous PLLA, PCL and PLCL samples at different degradation times.

PLCL was initially totally amorphous, displaying a single glass transition temperature ($T_g$) at ~17 ºC and no melting peak. However, as shown in Figure 1, the copolymer displayed a double $T_g$ behavior and a melting peak was observed at ~95 ºC after 3 days submerged in PBS. The first $T_g$ could be associated with the hybrid amorphous miscible lactide-caprolactone phase, whereas the second $T_g$ may be ascribed to the presence of phase separated amorphous lactide domains. As the time immersed in PBS increased the first $T_g$ moved toward lower values and the $X_c$ increased, indicating the migration of lactide sequences from the lactide-caprolactone miscible phase to the lactide crystalline domains. In this sense, the first $T_g$ had a value of 17 ºC on day 3 and dropped to 2 ºC on day 132, whereas $X_c$ increased from 1% on day 3 to 28% on day 132. The microstructure of this copolymer was characterized by nuclear magnetic resonance (NMR) in a previous study by our group [25]. According to this earlier study the copolymer has an average sequence length of L-lactide ($l_{LA}$) equal to 3.45 and a randomness character close to 1 (R = 0.92), indicating a random distribution of

sequences. This PLCL was able to maintain its amorphous character when it was stored at room temperature for a period up to 5 months. However, in the hydrolytic degradation study presented in this work, microstructural rearrangements occurred faster and lactide sequences were able to crystallize in few days due to the presence of plasticizing water and the higher mobility of shorter chains produced during the hydrolytic scission [26, 27],.

Figure 2 represents the evolution of $\ln M_w$ of non-porous PLLA, PCL and PLCL over degradation time. The experimental data follow the exponential relationship between molecular weight and degradation time, previously described in literature for polyesters degrading under bulk degradation, satisfactorily [28]:

$$\ln M_w = \ln M_{w0} - K_{Mw} \cdot t \quad (5)$$

$$t_{1/2} = \ln 2/K_{Mw} \quad (6)$$

where $M_w$ is the weight average molecular weight, $M_{w0}$ is the initial weight average molecular weight, $K_{Mw}$ is the apparent degradation rate and $t_{1/2}$ is the half degradation time.

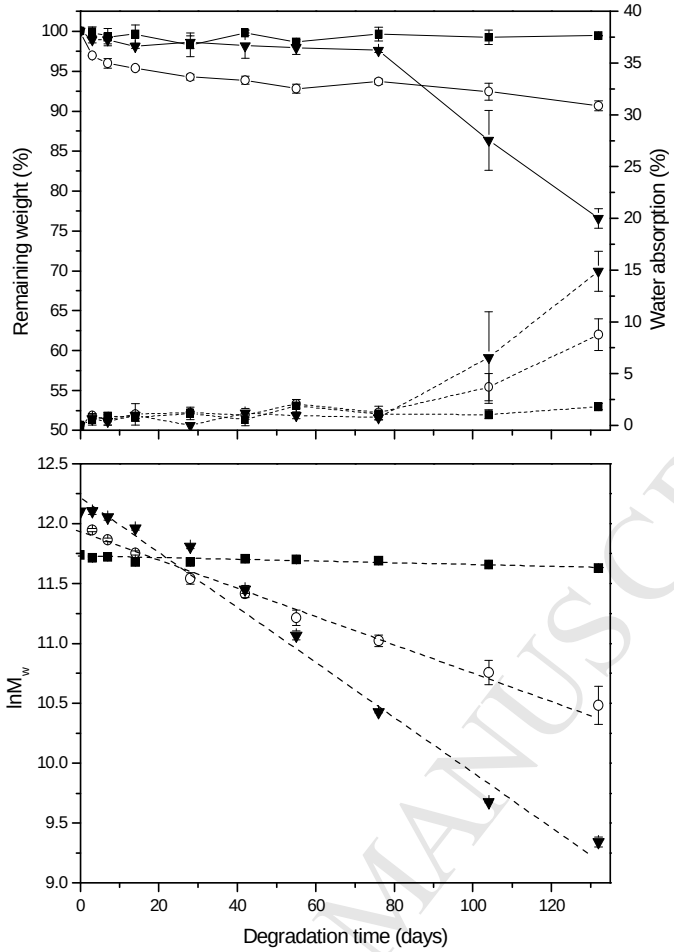


**Figure 2.** Evolution of remaining weight, water absorption and $lnM_w$ of non-porous PLLA (○), PCL (■) and PLCL (▼) samples at different degradation times.

The slope of each fitting curve was employed to calculate $K_{Mw}$ and corresponding $t_{1/2}$ of the studied materials. In this sense, the obtained $K_{Mw}$ values for PLLA, PCL and PLCL were respectively 0.0112, 0.0006 and 0.0227 $days^{-1}$ with corresponding $t_{1/2}$ of 62, 1155 and 31 days. The degradation rate of PCL was the slowest of the materials studied. In fact, $M_w$ of PCL dropped slightly from the initial value of ~125000 to 112000 g $mol^{-1}$ at day 132, whereas no mass loss was monitored during the course of the study. In this sense, the remaining mass of PCL films at the end of the study (day 132) was 99.5 ± 0.02%. One should bear in mind that the degradation of polyesters occurs by hydrolysis of the ester bonds and that crystalline regions in the polymer structure are more resistant to hydrolytic degradation than amorphous ones. Given its high crystallinity and the fact

that, of the materials studied, PCL has the lowest ester group density within its backbone, and so the results obtained were expected [29]. Malin *et al.* [30] observed no molecular weight decrease in PCL plates after being submerged in PBS at 37 ºC for up to 70 days, that is in accordance with the results obtained in this work.

In contrast, PLCL showed the fastest degradation rate of the materials studied. As shown in Figure 1, incorporation of caprolactone units disrupts the chain regularity of crystallisable lactide sequences, resulting in a material with reduced crystallinity, compared to PLLA and PCL. It is well known that water penetrates amorphous regions easier than crystalline ones, leading to a faster degradation of amorphous regions in comparison to crystalline domains [31]. For this reason, both highly crystalline PCL and PLLA displayed slower degradation rates than PLCL. Moreover, these hydrolytically highly resistant crystalline residues can remain within the body for years and cause a foreign-body reaction [32-34]. Therefore, bioresorbable polymers that are able to maintain their amorphous character during degradation are desirable for biomedical applications [13]. The mass of non-porous PLCL samples stayed almost constant until day 76. It then suffered a sharp mass reduction and was accompanied by an increase in water absorption. In this sense, remaining weight dropped from 97.6 ± 0.3% on day 76 to 76.6 ± 1.2% at day 132, whereas water absorption increased from 0.9 ± 0.3% to 14.9 ± 1.9% over the same period.

The mass of non-porous PLLA samples decreased in the first week to 96.0 ± 0.6% but during the period of the study any further changes observed were only minor, reaching 90.7 ± 0.6% on day 132. Water absorption of non-porous PLLA samples was maintained almost constant until day 76, when it reached a value of 1.2 ± 0.7%. Then, it increased sharply and took a value of 8.8 ± 1.6% at the end of the study.

*3.1.2. Hydrolytic degradation of porous samples*

The microstructural rearrangements described in Figure 1 for non-porous samples were also observed in porous counterparts (data not shown). In particular samples of PCL and PLCL showed very small differences between non-porous and porous samples in the calculated $X_c$ values, suggesting that the presence of pores had little effect on the aforementioned thermal transitions during hydrolytic degradation. In this sense, PCL reached 64% of $X_c$ for both non-porous and porous samples on day 132. As mentioned in the previous section, the $X_c$ of PLCL increased with degradation time and reached 28 and 25% for non-porous and porous samples, respectively, on day 132. In contrast, large differences were observed between non-porous PLLA samples and their porous counterparts. To illustrate this point, at the end of the study (day 132) the $X_c$ of non-porous PLLA was 58%, whereas $X_c$ of porous PLLA was 45%. The results obtained for PLLA suggest that degradation of porous and non-porous samples was occurring in a very different way. This hypothesis was confirmed when $K_{Mw}$ and $t_{1/2}$ values were calculated (Table 1).

**Table 1.** $K_{Mw}$, $t_{1/2}$ and remaining weight (on day 132) of the studied systems.

| | $K_{Mw}$ *(days$^{-1}$)* | $t_{1/2}$ *(days)* | *Remaining wt. (%)* |
|---|---|---|---|
| *Non-porous PLLA* | 0.0112 | 62 | 90.7 ± 0.6 |
| *Porous PLLA* | 0.0049 | 141 | 93.4 ± 0.6 |
| *Porous PLLA+BG* | 0.0123 | 56 | 68.3 ± 4.4 |
| *Non-porous PCL* | 0.0006 | 1155 | 99.5 ± 0.1 |
| *Porous PCL* | 0.0004 | 1733 | 97.4 ± 2.4 |
| *Porous PCL+BG* | 0.0005 | 1386 | 88.3 ± 0.6 |
| *Non-porous PLCL* | 0.0227 | 31 | 76.6 ± 1.2 |
| *Porous PLCL* | 0.0192 | 36 | 83.5 ± 2.6 |
| *Porous PLCL+BG* | 0.0170 | 41 | 81.5 ± 1.4 |

As can be seen in Table 1, porous samples degraded slower than non-porous samples. It should be noted that chain scission results in the formation of acidic by-products which, owing to their acidic nature, will enhance the rate of further hydrolysis [11]. In non-porous samples, the diffusion of these acidic by-products to the outside medium is hindered and the autocatalytic effect enhanced, leading to a faster degradation rate with regards to porous structures, where the diffusion of these by-products is facilitated [35, 36]. Particularly significant was the case of PLLA, which showed a large difference between the calculated $K_{Mw}$ and corresponding $t_{1/2}$ for non-porous and porous samples. In this sense, the $t_{1/2}$ of porous PLLA was 2.3 times longer than that of its non-porous counterpart. This fact may justify the differences observed in $X_c$ between non-porous and porous PLLA samples during degradation. In non-porous PLLA samples, shorter chains with higher mobility are produced as a result of the faster degradation. For this reason, they have a higher mobility and reorganization capability, leading to a higher $X_c$ value at the end of the study when compared to the less degraded porous samples.

Weight loss measurements confirmed the slower degradation of porous samples, compared to non-porous samples. In this sense, non-porous PLLA and PLCL presented a remaining weight of 90.7 ± 0.6 and 76.6 ± 1.2 respectively on day 132, whereas their porous counterparts showed 93.4 ± 0.6 and 83.5 ± 2.6. However, PCL samples did not suffer any significant weight losses during the course of the study due to its extremely slow degradation rate.

The results of hydrolytic degradation for samples filled with bioactive glass particles did not follow a general trend, making the interpretation of the results difficult. Ignoring the case of the PCL sample, where degradation rates were so small that comparison between the samples was meaningless, two opposing situations were observed in PLLA and PLCL. In the case of PLCL porous samples filled with bioactive glass particles, the

$K_{Mw}$ was slightly lower than in the unfilled porous PLCL counterpart ($K_{Mw}$ = 0.0170 $days^{-1}$ for a PLCL porous sample filled with bioactive glass compared to a $K_{Mw}$ = 0.0192 $days^{-1}$ for unfilled PLCL porous sample) indicating that the incorporation of bioactive glass slowed the hydrolytic degradation of the copolymer down. Blaker *et al.* [37] and Boccaccini *et al.* [38] found similar results for poly(D,L-lactide) (PDLLA) and poly(lactide-co-glycolyde) (PLGA) porous scaffolds filled with bioactive glass particles. It has been proposed that bioactive glass particles produce a rapid exchange of protons in the water for the alkali in the glass, providing a pH buffering effect that neutralizes the acidic degradation by-products produced during hydrolysis, thus preventing the autocatalytic effect. The case of PLLA samples is in clear contrast; with the incorporation of bioactive glass particles to porous PLLA samples the result was a faster degradation rate ($K_{Mw}$ = 0.0123 $days^{-1}$ for PLLA porous sample filled with bioactive glass compared to a $K_{Mw}$ = 0.0049 $days^{-1}$ for unfilled PLLA porous sample). This result is difficult to explain since most of the studies seen in the bibliography indicate that the incorporation of bioactive glass reduces the degradation rate of porous samples due to the aforementioned pH buffering effect. However, some authors [39, 40] have found that the incorporation of bioactive glass particles enhances water absorption which accelerates the ester hydrolysis of the polymer matrix. On the other hand, incorporation of bioactive glass particles slightly reduces the porosity of PLLA samples from 92.4 ± 0.3% to 89.9 ± 0.5%. Considering the significant effect porosity has on the degradation of PLLA, the slight decrease in porosity produced by the incorporation of bioactive glass particles may have hindered the diffusion of acidic by-products to the outside medium, enhancing the autocatalytic effect and accelerating the degradation of bioactive glass filled porous PLLA samples. Whatever the reason, as stated above, the

obtained results for porous PLLA samples filled with bioactive glass particles were totally unexpected.

Figure 3 displays remaining weight of unfilled and bioactive glass filled PLLA, PCL and PLCL porous samples as a function of immersion time in PBS. Samples containing bioactive glass suffered 8-10% weight loss during the first 14 days of immersion, this can be ascribed to the dissolution or loss of bioactive glass particles [37, 41]. Afterwards the weight of the samples stayed constant until day 76 for PLLA and day 104 for PLCL, when weight losses associated to polymer mass loss occurred. In the case of PCL samples, no additional weight losses associated with polymer degradation were seen due to the slow degradation rate of this polymer.

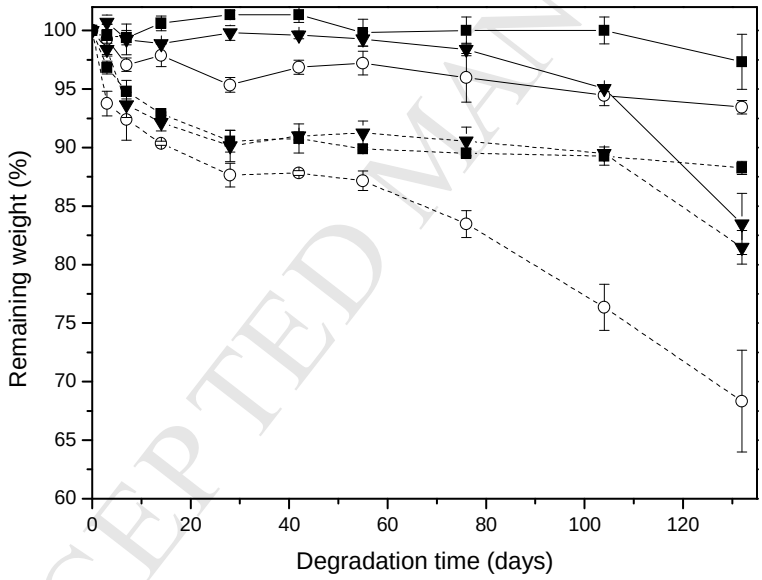


**Figure 3.** Evolution of remaining weight of unfilled (solid line) and bioactive glass filled (dashed line) porous PLLA (○), PCL (■) and PLCL (▼) samples at different degradation times.

The pH of the medium was also monitored during the hydrolytic degradation study. The medium containing unfilled porous samples displayed a pH value of ~7.2 which stayed more or less constant over degradation time, whereas the medium containing bioactive glass filled porous samples had pH values of ~7.4. Such a small difference may be related to the dissolution of alkaline ions from bioactive glass particles that locally

compensate for the acidification of the medium due to the release of acidic degradation by-products. Such a buffering effect is thought to be another benefit of using bioactive glass particles in composites with the aim of avoiding any possible inflammatory response due to the acidic degradation of the polymers [38].

### 3.2. Bioactivity study

The bioactivity study was carried out in PLLA scaffolds filled with 0, 15 and 30 vol.% of bioactive glass particles. In the SEM micrographs in Figure 4, the Ca-P depositions are clearly seen in the scaffolds containing bioactive glass. Moreover, the deposition occurred faster and to a greater extent as the particle content increased. Some Ca-P depositions were observed after 28 days submerged in SBF for the PLLA scaffold filled with 15 vol.% of bioactive glass (Figure 4c), whereas the surface of the PLLA scaffold filled with 30 vol.% of bioactive glass was almost completely covered by a Ca-P layer (Figure 4f) at the same time. On the contrary, the unfilled PLLA scaffold maintained its smooth surface and no depositions were observed.

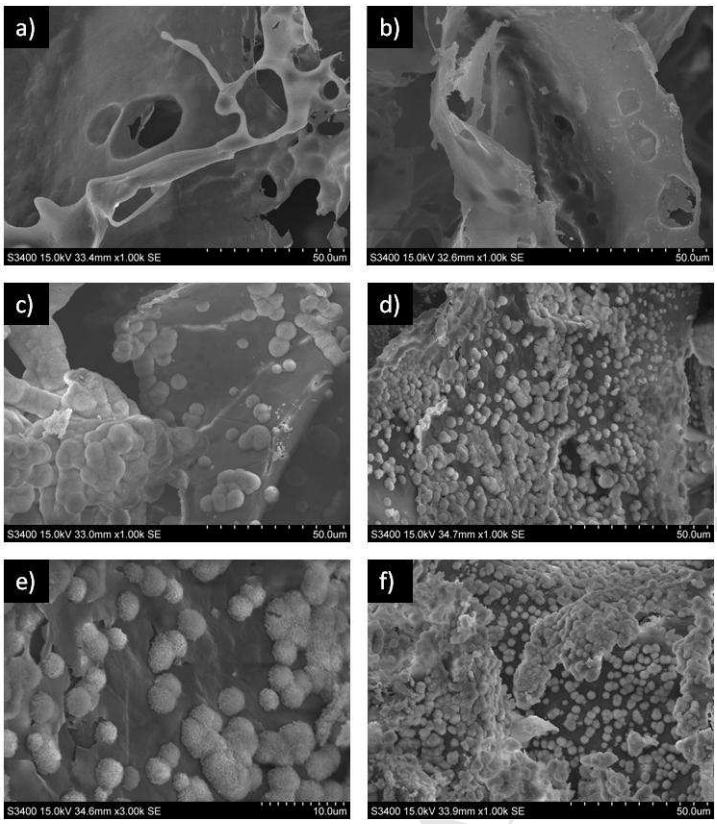


**Figure 4.** Scanning electron micrographs of an unfilled PLLA scaffold at day 0 (a) and after 28 days submerged in SBF (b); a PLLA scaffold filled with 15 vol.% of bioactive glass after 28 days submerged in SBF (c); a PLLA scaffold filled with 30 vol.% of bioactive glass after 14 days (d,e) or 28 days (f) submerged in SBF. (Original magnification x 1000 except in e), where the magnification was x 3000).

These results were confirmed by means of FTIR. As seen in Figure 5, the FTIR spectra of the scaffolds submerged for 0, 3, 7, 14 and 28 days indicate the growth of an apatite layer within the scaffold. The peaks at 874, 1420 and 1458 $cm^{-1}$ are indicative of the $\nu_2$ and $\nu_3$ vibrations of $CO_3^{2-}$. The sharp peaks at 564 and 606 $cm^{-1}$, which correspond to $\nu_4$ vibrations of $PO_4^{3-}$, indicated the apatite formation [42].

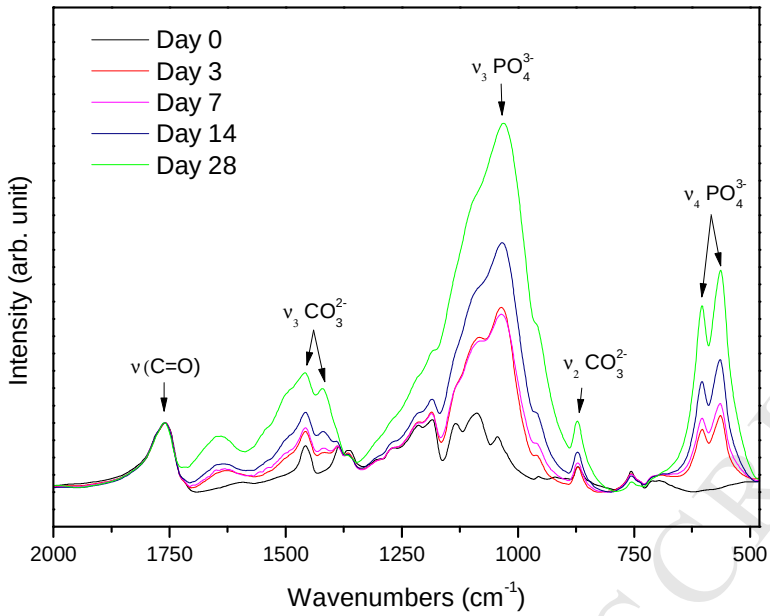


**Figure 5.** FTIR spectra of a PLLA scaffold filled with 30 vol.% of bioactive glass submerged for 0, 3, 7, 14 and 28 days in SBF.

Each of these peaks increased over incubation time with respect to the carbonyl peak at 1759 $cm^{-1}$, representing the growth of a carbonated apatite mineral. The carbonyl peak is characteristic of the polymer, whereas the vibrations of $PO_4^{3-}$ are characteristic of the apatite. The ratio of apatite/polymer, which can be estimated by the ratio of these peak areas, has been represented in Figure 6. As observed by SEM, the higher the bioglass content the faster the apatite formation.

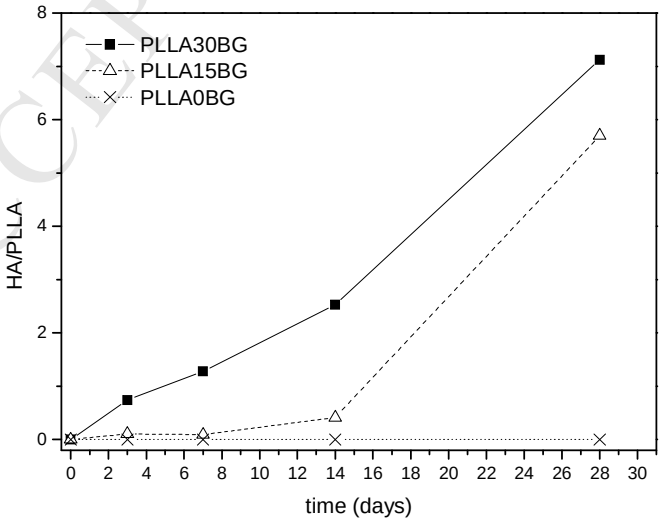


**Figure 6.** Ratio of apatite (HA) to PLLA for PLLA scaffolds filled with 0, 15 and 30 vol.% of bioactive glass as a function of immersion time in SBF, determined by the ratio of areas under the peaks in Figure 5.

Finally, to demonstrate the gradual crystallinity of the apatite forming on the foam surface over time in SBF, an XRD analysis was made (Figure 7). As can be seen, the intensities of apatite peaks (at 32º and 26º) increased with incubation time in the SBF compared to the PLLA peaks (at 17º and 19º).

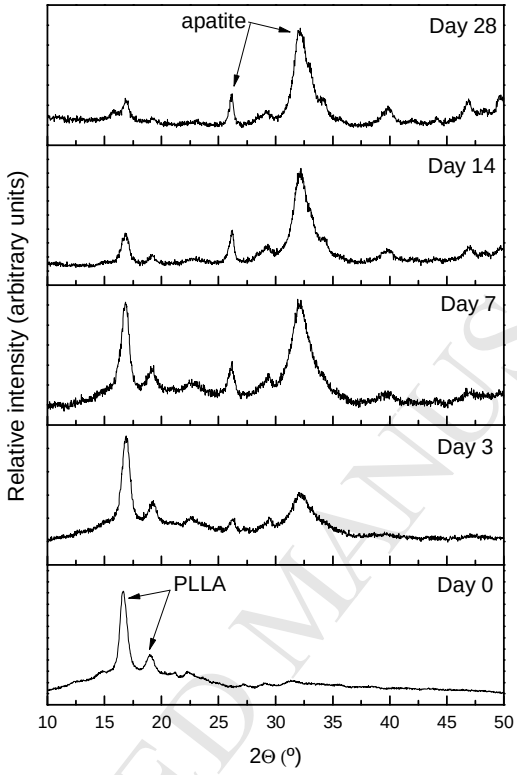


**Figure 7.** XRD patterns of a PLLA scaffold filled with 30 vol.% of bioactive glass after immersion in SBF for different times, showing the formation of crystalline apatite.

According to other studies these particles form an apatite layer that bonds chemically with living bone when they come into contact with body fluids or a mix of several solutions *in vitro*. The deposition of this layer starts with the formation of a silica gel layer on the surface of the bioactive particles, this provides chemisorption sites for $Ca^{2+}$ and $PO_4^{3-}$ thanks to its low isoelectric point and high surface area [14]. Finally, the crystallization of the amorphous $CaO\text{-}P_2O_5$ film takes place with the incorporation of $OH^-$ and $CO_3^{2-}$ (from solutions) to form a crystalline hydroxyl carbonate apatite layer. The results obtained confirmed that the deposition rate of the apatite layer increased with a higher amount of bioactive glass particles within the polymer matrix. This effect

has been reported by other authors [43]. However, they needed larger quantities of bioactive glass (50 wt.% ≈ 25 vol.%) and longer periods (21 days) for the formation of the apatite layer to be observed. Jaakkola *et al.* [44] worked with PLCL samples loaded with 40 and 70 wt.% of bioactive glass of various sizes (<45 µm and 90-315 µm). So this study concluded that the higher the glass content and the glass surface/volume ratio in the matrix, the faster the Ca-P formation. In our case, even the scaffold filled with the lowest bioactive glass content (15 vol.%) showed the precipitation of the apatite layer after just 14 days. In the case of the scaffold with a higher content of bioactive glass (30 vol.%), the apatite layer was observed after 3 days submerged in SBF. All these results indicated the high bioactivity of the composite materials produced and confirmed their potential as bone tissue-engineering scaffolds.

## 4. Conclusions

This study investigated the hydrolytic degradation of non-porous and porous PLLA, PCL and PLCL samples. The results obtained showed the following sequence in the degradation rate (from the fastest to the slowest): PLCL>PLLA>PCL. PCL, owing to its high crystallinity and the lowest ester group density within its backbone, experienced the slowest degradation rate and no mass loss was monitored during the course of the study. PLCL, which was initially totally amorphous but turned semicrystalline during the period of the study, showed the fastest degradation rate owing to its reduced crystallinity compared to PLLA and PCL.

Porous PLLA, PCL and PLCL samples degraded more slowly than their non-porous counterparts. The porous structure enables the diffusion of acidic by-products, which reduces the autocatalytic effect. Particularly relevant was the large difference between PLLA porous and non-porous samples. For example, $t_{1/2}$ calculated for porous PLLA

samples was 2.3 times higher than that of non-porous PLLA. The incorporation of bioactive glass particles delayed the degradation rate of PLCL, probably due to the pH buffering effect provided by bioactive glass particles that neutralize the acidic degradation by-products and prevent the autocatalytic effect. However, unexpected results were found for bioactive glass filled porous PLLA. In this case, incorporation of bioactive glass particles accelerated the degradation rate of the polymer matrix.

The pH of the medium was maintained slightly higher in the case of bioactive glass filled samples. Such an effect has been considered to be another benefit of using bioactive glass particles in composites so as to avoid any possible inflammatory response due to the acidic degradation of the polymers.

Moreover, the bioactivity of PLLA porous scaffolds filled with 0, 15 and 30 vol.% of bioactive glass particles was studied in this work. The results obtained confirmed apatite layer formation on the surface of bioactive glass filled porous samples. What is more, this deposition occurred faster and to a greater extent as the particle content within the polymer matrix increased.

In summary, it can be concluded that 3-dimensional scaffolds with different degradation rates have been successfully created. In principle, the degradation rate of the scaffold should match the rate of tissue formation. Therefore, for specific applications great care must be taken when deciding on which material is to be employed as it is morphology dependent. In addition, the bioactivity study confirmed the high bioactivity of the composite materials employed and assessed their potential as bone tissue engineering scaffolds.

## Acknowledgment

The authors are thankful for funds from the Basque Government, Department of Education, Universities and Research (GIC13/161-IT-632-13) and Dept. of Health (ref. 2007111061, SAN07/01). A. L. thanks the University of the Basque Country (UPV-EHU) for a pre-doctoral grant.

## References

1. Langer R, Vacanti JP. Tissue Engineering. Science 1993; 260: 920-926.
2. Schmitz JP, Hollinger JO. The Critical Size Defect as an Experimental Model for Craniomandibularfacial Nonunion. Clincial Orthopaedics and Related Research 1986; 205: 299-308.
3. Honma T, Itagaki T, Nakamura M, Kamakura S, Takahashy I, Echigo S, Sasano Y. Bone Formation in Rat Calvaria Ceases within a Limited Period Regardless of Completion of Defect Repair. Oral Diseases 2008; 14: 457-464.
4. Damien C, Parson R. Bone Graft and Bone Graft Substitutes: a Review of Current Technology and Applications. Journal of Applied Biomaterials 1991; 2: 187-208.
5. Petite H, Viateau V, Bensaïd W, Meunier A, de Pollak C, Bourguignon M, Oudina K, Sedel L, Guillemin G. Tissue-Engineered Bone Regeneration. Nature Biotechnology 2000; 18: 959-963.
6. Bruder SP, Kraus KH, Goldberg VM, Kadiyala S. The Effect of Implants Loaded with Autologous Mesenchymal Stem Cells on the Healing of Canine Segmental Bone Defects. Journal of Bone and Joint Surgery 1998; 80A: 985-996.
7. Sikavitsas VI, van den Dolder J, Bancroft GN, Jansen JA, Mikos AG. Influence of the *In Vitro* Culture Period on the *In Vivo* Performance of Cell/Titanium Bone

Tissue-Engineered Constructs using a Rat Cranial Critical Size Defect Model. Journal of Biomedical Materials Research 2003; 67A: 944-951.

8. Liao SS, Cui FZ, Zhang W, Feng QL. Hierarchically Biomimetic Bone Scaffold Materials: Nano-HA/Collagen/PLA Composite. Journal of Biomedical Materials Research 2004; 69B: 158-165.
9. Lendeckel S, Jödicke A, Christophis P, Heidinger K, Wolff J, Fraser JK, Hedrick MH, Berthold L, Howaldt HP. Autologous Stem Cells (Adipose) and Fibrin Glue used to Treat Widespread Traumatic Calvarial Defects: Case Report. Journal of Cranio-Maxillofacial Surgery 2004; 32: 370-373.
10. Hutmacher DW. Scaffolds in Tissue Engineering Bone and Cartilage. Biomaterials 2000; 21: 2529-2543.
11. Edlund U, Albertsson AC. Polyesters Based on Diacid Monomers. Advanced Drug Delivery Reviews 2003; 55: 585-609.
12. Fernández J, Larrañaga A, Etxeberría A, Sarasua JR. Effects of Chain Microstructures and Derived Crystallization Capability on Hydrolytic Degradation of Poly(L-lactide/ε-caprolactone) Copolymers. Polymer Degradation and Stability 2013; 98: 481-489.
13. Fernández J, Larrañaga A, Etxeberría A, Sarasua JR. A New Generation of Poly(Lactide/ε-caprolactone) Polymeric Biomaterials for Application in the Medical Field. Journal of Biomedical Materials Research Part A. *In press.*
14. Hench LL, Wheeler DL, Greenspan DC. Molecular Control of Bioactivity in Sol-Gel Glasses. Journal of Sol-Gel Science and Technology 1998;13:245-250.
15. Cao W, Hench LL. Bioactive Materials. Ceramics International 1996; 22: 493-507.

16. Hench LL. The Story of Bioglass. Journal of Materials Science: Materials in Medicine 2006;17:967-978.

17. Xynos ID, Edgar AJ, Buttery LDK, Hench LL, Polak JM. Gene-Expression Profiling of Human Osteoblasts Following Treatment with the Ionic Products of Bioglass 45S5 Dissolution. Journal of Biomedical Materials Research 2001; 55: 151-157.

18. Gerhardt LC, Widdows KL, Erol MM, Burch CW, Sanz-Herrera JA, Ochoa I, Stämpfli R, Roqan IS, Gabe S, Ansari T, Boccaccini AR. The Pro-Angiogenic Properties of Multi-Functional Bioactive Glass Composite Scaffolds. Biomaterials 2011; 32: 4096-4108.

19. Kokubo T, Takadama H. How Useful is SBF in Predicting *In Vivo* Bone Bioactivity?. Biomaterials 2006; 27: 2907-2915.

20. Blaker J, Gough JE, Maquet V, Notingher I, Boccaccini AR. *In Vitro* Evaluation of Novel Bioactive Composites Based on Bioglass-Filled Polylactide Foams for Bone Tissue Engineering Scaffolds. Journal of Biomedical Materials Research 2003; 67A: 1401-1411.

21. Sarasua JR, Prud´homme RE, Wisnieski M, Le Borgne A, Spassky N. Crystallization and Melting Behaviour of Polylactides. Macromolecules 1998; 31: 3895-3905.

22. Gong Y, Zhou Q, Gao C, Shen J. *In Vitro* and *In Vivo* Degradability and Cytocompatibility of Poly(L-lactic Acid) Scaffold Fabricated by a Gelatin Particle Leaching Method. Acta Biomaterialia 2007; 3: 531-540.

23. Lu L, Peter SJ, Lyman MD, Lai HL, Leite SM, Tamada JA, Vacanti JP, Langer R, Mikos AG. *In Vitro* Degradation of Porous Poly(L-lactic Acid) Foams. Biomaterials 2000; 21: 1595-1605.

24. Labet M, Thielemans W. Synthesis of Polycaprolactone: a Review. Chemical Society Reviews 2009; 38: 3484-3504.

25. Fernández J, Etxeberría A, Ugartemendia JM, Petisco S, Sarasua JR. Effect of Chain Microstructures on Mechanical Behavior and Aging of a Poly(L-lactide-co-ε-caprolactone) Biomedical Thermoplastic-Elastomer. Journal of the Mechanical Behavior of Biomedical Materials 2012; 12: 29-38.

26. Saha SK, Tsuji H. Enhanced Crystallization of Poly(L-lactide-co-ε-caprolactone) in the Presence of Water. Journal of Applied Polymer Science 2009; 112: 715-720.

27. Saha SK, Tsuji H. Effects of Rapid Crystallization on Hydrolytic Degradation and Mechanical Properties of Poly(L-lactide-co-ε-caprolactone). Reactive&Functional Polymers 2006; 66: 1362-1372.

28. Wu L, Ding J. Effects of Porosity and Pore Size on *In Vitro* Degradation of Three-Dimensional Porous Poly(D,L-lactide-co-glycolide) Scaffolds for Tissue Engineering. Journal of Biomedical Materials Research 2005; 75: 767-777.

29. Han X, Pan J. Polymer Chain Scission, Oligomer Production and Diffusion: A Two-Scale Model for Degradation of Bioresorbable Polyesters. Acta Biomaterialia 2001; 7: 538-547.

30. Malin M, Hiljanen-Vainio M, Karjalainen T, Seppälä J. Biodegradable Lactone Copolymers. II. Hydrolytic Study of ε-caprolactone and Lactide Copolymers. Journal of Applied Polymer Science 1996; 59: 1289-1298.

31. Jeong SI, Kim BS, Kang SW, Kwon JH, Lee YM, Kim SH, Kim YH. *In Vivo* Biocompatibility and Degradation Behavior of Elastic Poly(L-lactide-co-ε-caprolactone) scaffolds. Biomaterials 2004; 25: 5939-5946.

32. Bergsma JE, de Bruijin WC, Rozema FR, Bos RRM, Boering G. Late Degradation Tissue Response to Poly(L-lactide) Bone Plates and Screws. Biomaterials 1995; 16: 25-31.

33. Tams J, Rozema RF, Bos RRM, Roodenburg JLN, Nikkels PGJ, Vermey A. Poly(L-lactide) Bone Plates and Screws for Internal Fixation of Mandibular Swing Osteotomies. International Journal of Oral and Maxillofacial Surgery 1996; 25: 20-24.

34. Tsuji H, Ikarashi K. *In Vitro* Hydrolysis of Poly(L-lactide) Crystalline Residues as Extended-Chain Crystallites. Part I: Long-Term Hydrolysis in Phosphate-Buffered Solutions at 37 ºC. Biomaterials 2004; 25: 5449-5455.

35. Pamula E, Menaszek E. *In Vitro* and *In Vivo* Degradation of Poly(L-lactide-co-glycolide) Films and Scaffolds. Journal of Materials Science: Materials in Medicine 2008; 19: 2063-2070.

36. Dorati R, Colonna C, Genta I, Modena T, Conti B. Effect of Porogen on the Physico-Chemical Properties and Degradation Performance of PLGA Scaffolds. Polymer Degradation and Stability 2010; 95: 694-701.

37. Blaker J, Nazhat SN, Maquet V, Boccaccini AR. Long-Term *In Vitro* Degradation of PDLLA/Bioglass Bone Scaffolds in Acellular Simulated Body Fluid. Acta Biomaterialia 2011; 7: 829-840.

38. Boccaccini AR, Maquet V. Bioresorbable and Bioactive Polymer/Bioglass Composites with Tailored Pore Structure for Tissue Engineering Applications. Composites Science and Technology 2003; 63: 2417-2429.

39. Rich J, Jaakkola T, Tirri T, Närhi T, Yli-Urpo A, Seppälä J. *In Vitro* Evaluation of Poly(ε-caprolactone-co-DL-lactide)/Bioactive Glass Composites. Biomaterials 2002; 23: 2143-2150.

40. Wang Y, Liu L, Guo S. Characterization of Biodegradable and Cytocompatible Nano-Hydroxyapatite/Polycaprolactone Porous Scaffolds in Degradation *In Vitro*. Polymer Degradation and Stability 2010; 95: 207-213.

41. Orava E, Korventausta J, Rosenberg M, Jokinen M, Rosling A. *In Vitro* Degradation of Porous Poly(DL-lactide-co-glycolide) (PLGA)/Bioactive Glass Composite Foams with a Polar Structure. Polymer Degradation and Stability 2007; 92: 14-23.

42. Kontonasaki E, Zorba T, Papadopoulou L, Pavlidou E, Chatzistavrou X, Paraskevopoulos K, Koidis P. Hydroxy Carbonate Apatite Formation on Particulate Bioglass *In Vitro* as a Function of Time. Crystal Research Technology 2002; 37: 1165-1171.

43. Lu HH, Tang A, Oh SC, Spalazzi JP, Dionisio K. Compositional Effects on the Formation of a Calcium Phosphate Layer and the Response of Osteoblast-Like Cells on Polymer-Bioactive Glass Composites. Biomaterials 2005; 26: 6323-6334.

44. Jaakkola T, Rich J, Tirri T, Närhi T, Jokinen M, Seppälä J, Yli-Urpo A. In Vitro Ca-P Precipitation on Biodegradable Thermoplastic Composite of Poly(ε-caprolactone-co-DL-lactide) and Bioactive Glass (S53P4). Biomaterials 2004; 25: 575-581.